Talanta 223 (2021) 121795

Contents lists available at ScienceDirect

Talanta

journal homepage: www.elsevier.com/locate/talanta

Direct solid sampling for speciation of Zn^{2+} and ZnO nanoparticles in cosmetics by graphite furnace atomic absorption spectrometry

J.C. García-Mesa [a], P. Montoro-Leal [a], A. Rodríguez-Moreno [b], M.M. López Guerrero [a,**], E. I. Vereda Alonso [a,*]

[a] Department of Analytical Chemistry, Faculty of Sciences, University of Malaga, 29071, Málaga, Spain
[b] Department of Computer Architecture, Higher Technical School of Computer Engineering, University of Málaga, 29071, Málaga, Spain

ARTICLE INFO

Keywords:
ZnO nanoparticles
Eye shadow
Direct solid sampling
HR-CS-GFAAS

ABSTRACT

The application of nanoparticles (NPs) in science and technology is a fast growing field. Therefore, reliable and straightforward analytical methods are required for their fast determination in different types of samples. This work investigates a method that enables the determination of ZnO NPs, discriminating them from ionic zinc in cosmetic samples. The method is based on direct solid sampling high-resolution continuum source electrothermal atomic absorption spectrometry (SS-HR-CS-GFAAS), and has been applied to determination of ZnO NPs, Zn^{2+} and total Zn in eye shadow samples. In this work the deconvolution of the atomization peak and the calibration by standard additions have been done in order to discriminate and quantify ionic zinc and ZnO NPs. A Zn wavelength with low sensitivity was selected. The proper optimization of the graphite furnace temperature program, minimizing the mineralization of the sample matrix, enables different atomization profiles between the different chemical species of the analyte. Two multiple response surface designs have been used in order to optimize the adequate furnace program to achieve our aims. All the optimization experiments were performed using a sample of eye shadow. Further, a method for the determination of total Zn by direct solid sampling with calibration by aqueous standards, was also optimized. The optimized method was successfully applied to the determination of ionic Zn and ZnO NPs in different eye shadow samples, and has been validated by recovery assays, obtaining recovery percentages between 80 and 125%. Total Zn concentration in the solid samples was validated by the determination of total Zn by direct solid sampling and by the analysis of the same eye shadow samples digested in microwave oven.

1. Introduction

Metallic nanoparticles (NPs) are widely used in numerous industrial and medical applications. Fields of application include amongst other cosmetics, clothes, paints, food packaging, optics and medical devices [1,2]. This great variety of applications is due to their unique and exceptional physical and chemical properties: high surface-to-volume ratio, high surface reactivity, high stability, facility to cross the cellular membranes to enter in cells and to interact with proteins. However, the same unique properties that make metallic NPs so promising in industry and medicine could make them potentially toxic [3,4]. This is the reason why several studies are being carried out on their environmental impact and their possible effects on human health [5–7], and regulatory agencies are becoming more aware of this issue [8]. There are already some regulation in the European Union, as an example, food ingredients require to be identified when they are present in the nanoform [9].

The global cosmetic industry grows at a very high rate, by 4.5% annually [10]. The cosmetic market generated around 40 billion US$ in 2012 [11]; and the retail sales price in Europe was 72.5 billion € in 2014 mainly in Germany, France, UK, Italy and Spain [12]. Millions of people benefit daily from the use of cosmetic and the nanotechnology is widely used in this industry. A high number of cosmetics which contain NPs are considered of high value-added. Furthermore, products that use NPs provide better texture, spread ability, and UV protection [13]. However, as has been said before, NPs may also be a threat to human health as well as the environment. Most of these products do not indicate whether the product includes NPs, which means that consumers have no idea

* Corresponding author.
** Corresponding author.
E-mail addresses: mmlopez@uma.es (M.M. López Guerrero), eivereda@uma.es (E.I. Vereda Alonso).

https://doi.org/10.1016/j.talanta.2020.121795
Received 11 August 2020; Received in revised form 15 October 2020; Accepted 19 October 2020
Available online 21 October 2020

whether they are being exposed to nanomaterials. These NPs could penetrate the body becoming systematically available and eventually being accumulated in secondary target organs [14]. Thus, the regulation (EC) No 1223/2009, the European parliament mandated the labeling of cosmetics that include NPs, starting on July 11, 2013 [15]. This regulation stablishes that the presence of a nanomaterial in a cosmetic product must be explicitly indicated and notified to the European Commission. The notification must contain, among others, the following information: an identification of the nanomaterial, including its chemical name and other descriptors specified in the regulation and a specification of the nanomaterial, including its particle size and its physical and chemical properties.

Cosmetic products can be divided into several categories, such as makeup for children and adults, and include corrective facials, blush, eye shadow, lipstick, between others. Eye shadows are sold as anhydrous creams, sticks, emulsions, pencils, and as pressed powders, and they are available in different colors. They are applied in the periocular area, the area around the eyes. This area is the thinnest facial skin, therefore where there is more risk of percutaneous adsorption of the pigments, toxic elements and NPs. Eye shadows are composed by calcium carbonate, kaolin, titanium dioxide, zinc oxide, pigments, among others [11]. According to the International Cooperation on Cosmetic Regulations (ICRR), TiO_2 and ZnO NPs are used as inorganic UV filters in numerous personal care products [16], including eye shadows. ZnO NPs present also enhanced antimicrobial properties; this is the reason because ZnO particles have been shown to be one of the most harmful NPs in aquatic exposures [17]. However, in other aquatic tests, the toxicity of ZnO NPs can be attributed to the solubilized metal from the NPs in solution and not from ZnO NP forms [18]. There are few studies about the ZnO NPs toxicity [18,19]. Anyway, these studies agree that chronic toxicity of nanoparticulate and ionic zinc is different. On the other hand, chemical stability studies of Ag and ZnO NPs in the presence of mineral suspensions indicated that while no change were produced in Ag NPs during several months, ZnO NPs rapidly dissociated within 1 day [20]. In this context, the development of analytical methods rapid, simple, sensitive and selective, capable of characterizing and determining of ZnO NPs as well as discrimination from ionic form (speciation) in cosmetic samples are important.

To date, there are few studies on the determination of ZnO in cosmetics. Some of them, dissolve the sample totally, before the analysis by Flame Atomic Absorption Spectrometry (FAAS) or Inductively Coupled Plasma Optical Emission Spectrometry (ICP-OES); e.g. by a combination of dry (250 °C) and wet digestion with HCl 37% [21] or HNO_3–HCl–HF at 125-130 °C for 2 h [22]. In this last work, Zn is also determined in slurry emulsions of the sunscreen cream at 1% (m/v) in 0.5 M HNO_3 and 0.5% Triton X-100 as surfactant. The employ of stabilized suspensions is the other form to determinate ZnO in cosmetics, Salvador et al. [23] proposed emulsification in water with a non-ionic tensioactive (Nemol K-39) and isobutyl methyl ketone, followed by Zn determination by FAAS. Lu at al [13]. used emulsions of 0.04 g or more of the sunscreen powder in 1% Triton X-100 which were analysed by single particle-inductively coupled plasma mass spectrometry (SP-ICP-MS).

Similar sample treatments and techniques are employed for other determinations in cosmetic samples. Total element analysis is generally performed after matrix destruction, but due to the presence of refractory components in cosmetics, extreme conditions for the dissolution to give a clear solution are needed, and conventional procedures are based on dry ashing or wet digestion [24] often assisted by microwave energy. Detection is usually performed by ICP-OES [22] and ICP-MS [25,26]. Unfortunately, the matrix destruction carries risks of altering the original form and size in which the NPs are found in the sample, and considering the extreme conditions necessary, the digestion also possibilities their dissociation. Nowadays, there are a considerable amount of techniques available for characterizing nanomaterials [27], e.g., differential centrifugal sedimentation (DCS), nanoparticle tracking analysis (NTA), dynamic light scattering (DLS), static light scattering (SLS), scanning electron microscopy (SEM) and transmission electron microscopy (TEM). However, these techniques have significant limitations, such as cost, time of analysis, lack of element specificity, incompatibility with some sample matrices. Single particle (SP)-ICP-MS enables the characterization of metallic NPs in samples with complex matrices but SP-ICP-MS needs to work with stabilized suspensions of the samples. This implies that an extraction technique is necessary to distinguish solubilized metal from the NPs. Cloud point extraction (CPE) and solid phase extraction (SPE) approaches are capable of efficient speciation metal ion/metallic NPs [28]. Nevertheless, re-dispersion or elution of metallic NPs from the solid phase prior to analysis requires in some cases time-consuming steps or harsh conditions risking unintended species transformation [29]. Alternatively, graphite furnace atomic absorption spectrometry (GFAAS) has been used for nanoparticle characterization, particularly when high-resolution continuum source (HR CS) devices are employed for the direct analysis of solid samples. The first report on NP identification using an AAS technique was conducted by Gagné et al. [30], in this study an increase in the atomization temperature for Ag NPs in front to Ag ions was observed, this increase in the atomization temperature was also observed with the increase in the particle size of Ag NPs. HR- CS-GFAAS with solid sampling (SS) has shown great potential in direct analysis of solid samples and complex material [31], taking advantage of the no-necessity of sample pretreatment. Recently, SS-HR-CS-GFAAS was employed by our research group to develop a new strategy of evaluating the area and the upslope of the atomization signals (atomization rate (k_{at})) for a line of Fe with low sensitivity in the determination of both the iron concentration and average particle size in solid magnetic NPs [32]. For speciation studies metal ion/metallic NPs, in direct analysis of solid samples HR-CS-GFAAS, Feichtmeier and Leopold [2,33] have obtained results indicating the possibility to differentiate between nanoparticles and ionic species of Ag from the evaluation of atomization delays (t_{ad}). Resano at al [34] after a proper optimization of the furnace program also observed different atomization profiles for ionic Au and Au NPs. Moreover, the time of appearance of the maximum peak height was related to the particle size, because the atomization of larger particles is delayed in time (t_{ad}). However, quantification of mixtures of NPs and ionic species seems to be more problematic, and a proper deconvolution of overlapping peaks is needed.

In this work, a new method that enables the determination of the concentration of ZnO NPs, discriminating them from ionic zinc has been developed. Also, a method for the direct determination of total content of zinc through calibration with aqueous standards was developed. Both methods were based on SS-HR-CS-GFAAS, and have been applied to determination of Zn^{2+}, ZnO NPs and total Zn concentration, in pressed powders eye shadow samples. The purpose of this work is to confirm that it is possible the direct speciation of metallic NPs through SS-HR-CS-GFAAS and a suitable deconvolution program.

2. Experimental

2.1. Reagents, standards and samples

High purity reagents and standards were used in all experiments. Doubly de-ionized water (18 MΩ cm) obtained from a Milli-Q water system (Millipore, Bedford, MA, USA) was used throughout. Zn ionic standard solutions were prepared immediately prior to use by appropriate dilution of a Zn(II) stock standard 1000 mg/L (Merck, Darmstadt, Germany). Solid calibration standards were prepared by dilution of solid standards 49/49%(wt) ZnO/TiO_2 UV Shielding Powder 50 nm NPs (US Research Nanomaterials, Inc., Houston, USA) with graphite powder 99.9% (Sigma-Aldrich, St. Louis, USA) and homogenisation by vortex during 10 min. Compact powder eye shadow samples of several brands and different colors were purchased in cosmetic shops in Málaga, Spain. Concentrated nitric acid and hydrogen peroxide (Merck, Darmstadt, Germany) were also used.

2.2. Instrumentation

A high resolution continuum source graphite furnace atomic absorption spectrometer ContrAA 700 (Analytik Jena AG, Jena, Germany), equipped with an autosampler SSA 600 for solid sampling, with an integrated microbalance with a readability of 1 mg (Sartorius, Goettingen, Germany), was used in all experiments in this work. The optical system comprises a xenon short arc lamp (GLE, Berlin, Germany) operating in "hot-spot" mode as the radiation source, a high-resolution double echelle monochromator (DEMON) and a linear CCD array detector with 588 pixels, 200 of which are used for analytical purposes (monitoring of the analytical signal and BG correction) while the rest are used for internal functions, such as correcting for fluctuations in the lamp intensity. Transversely heated pyrolytic graphite tubes with graphite platforms to introduce solid samples were employed for the different experiments. The typical uncertainty (standard deviation) of mass measurements ($n = 10$) is 1 mg or lower. Data evaluation was achieved with the software ASPECT CS 2.1.2.0 (Analytik Jena AG, Jena, Germany) and Multipak 9.0 Data Reduction Software for AES and XPS (Physical Electronics, Chanhassen, MN, USA). The optimum instrumental operation conditions were summarized in Table 1.

For purposes of validation, the eye shadow samples were digested using a microwave oven Multiwave 3000 (Anton Paar, Graz, Austria).

2.3. Optimization strategy

In this work, it was thought that multiple response experiments designs would be suitable for the furnace programme optimization. As a first step, preliminary experiments were carried out in order to stablish the lower and upper values of the furnace programme variables. During these experiments, multiple peaks were observed for samples (eye shadow samples produced two peaks) and only one peak was observed for ionic zinc standard and for solid ZnO NPs standard. This fact led us to think that speciation analysis would be possible. Three response functions were chosen to maximize the signal of the two peaks obtained for the sample and the distance (Spectr. no.) between them. Two central composite surfaces designs [35] were performed for optimization of the parameters. The lower and upper values for both designs and the response functions used, are given in Table 2. In the first design, the variables to be optimized were pyrolysis and atomization temperatures and atomization ramp; for this design, as mentioned above, three response function were used: Height peak 1/mass, Height peak 2/mass and distance between peaks (Spectr. no.). The signals of both peaks were divided by the mass weighted of sample due to difficulty to weigh the same sample amount every time. In the second design, pyrolysis and atomization hold time and pyrolysis ramp were optimized, in this case only the response function: distance between peaks (Spectr. no.) was used. The same eye shadow sample was used for all the experiments.

Table 1
HR CS GFAAS optimized instrumental parameters.

Wavelength			307.590 nm	
Number of detector pixels summed per line			3 (4.20 p.m.)	
Sample weight			0.100–0.300 mg	
Temperature program				
Step	Temperature (°C)	Ramp (°C s^{-1})	Hold time (s)	Ar gas flow (L min^{-1})
Drying	80	6	20	2.0
Drying	90	3	40	2.0
Drying	110	5	20	2.0
Pyrolysis	150/300[a]	3/50[a]	6/20[a]	2.0
Gas adaptation	150	0	5	0.0
Atomization	1350	1000/1500[a]	3	0.0
Cleaning	2450	500	4	2.0

[a] Conditions for solid sampling analysis of total zinc.

Table 2
Lower and upper values for design 1 and 2; and responses for the multivariate optimization of graphite furnace temperature programme.

Design 1	Lower	Upper	Response
Pyrolysis temperature (°C)	200	700	Height peak 1/mass
Atomization ramp (°C s^{-1})	800	1200	Height peak 2/mass
Atomization temperature (°C)	1200	1500	Distance between peaks (spectr. no.)
Desing 2			
Pyrolysis ramp (°C s^{-1})	5	40	Distance between peaks (spectr. no.)
Pyrolysis hold time (s)	10	50	
Atomization hold time (s)	3	6	

Each experiment was repeated three times, at least. The response surfaces designs chosen were central composited designs, these designs included a total of $2^k + 2\ x\ k + n$ runs, where k is the number of parameters to optimize ($k = 3$), 2^3 are the points from the factorial experiments carried out at the corners of the cube and 2×3 are the points carried out on the face centred star. The repetition of the centre point was used to estimate the experimental error ($n = 2$) in both designs. The resulting 16 experiments for each design were randomly performed.

The experimental data were processed by using the Statgraphics Centurion software (version 16.1.11 for Windows) (Statgraphics Technologies, Inc., The Plains, VA, USA). For the designs, the significance of the effects was checked by analysis of the variance (ANOVA) and using p-value significance levels. This value represents the probability of the effect of a factor being solely due to random error. This, if the p-value is less than 5%, the effect of the corresponding factor is significant.

The rest of variables were optimized with one-at-a-time (univariate) method, changing one parameter at a time while keeping the others constant.

The optimized temperature programme was partially modified in the pyrolysis and atomization steps by a univariate mode for the optimization of the method for the analysis of total zinc in eye shadow samples by solid sampling analysis with aqueous standards.

2.4. Procedure for analysis of cosmetic samples

Samples were directly analysed without hardly preparation steps, just a drying in an oven at 95 °C to constant weight and then a homogenisation by vortex for 10 min. The humidity of the samples was between 0.3 and 0.4% w/w. The solid sampling device used allows for automatic weighing and transporting of the samples into the furnace. First, a graphite platform was transported to the microbalance using a pair of tweezers. After taring, an appropriate amount of the sample (between 0.100 and 0.300 mg) was placed on the platform and weighed. Then, the platform was transferred to the graphite furnace and subjected to the temperature program (Table 1). All operations were fully controlled by the computer, except for the deposition of the sample on the platform, which was manually undertaken. The signal obtained was exported to comma-separated values (CSV) file format to be deconvoluted using the Multipak software. The integrated area for each peak was used to speciation analysis of Zn^{2+}/ZnO NPs in the eye shadow samples. The integrated area (3 pixels) for the only peak obtained was used to the solid sampling analysis of total zinc in the eye shadow samples. In all cases, the integrated area was divided by the mass of sample weighed.

Also, the eye shadow samples were digested with an acid treatment in microwave oven. For that, microwave digestion methods used by other authors for cosmetic analysis were studied [10,12] and a similar procedure to these was selected: a volume of 1.5 mL concentrated nitric acid and 0.5 mL of 30% hydrogen peroxide were poured to an accurately weighed amount of 0.10–0.15 g into a digest vessel, then the vessels with the samples were put into the microwave oven to 900 W for 30 min, at this power, a temperature of 200 °C was reached After cooling, the digested samples were evaporated to dryness to eliminate excess of

acids, and diluted with de-ionized water in 25 mL volumetric flasks. Aliquots of 20 μL of these samples were injected in the graphite tube for the analysis of total Zn.

3. Results and discussion

3.1. Wavelength selection

Zinc shows only two analytical lines in atomic absorption spectrometry, 213.857 and 307.590 nm, being the first around one hundred times more sensible than the second one. Since, Zn concentration in eye shadow samples is high (%, w/w), the less sensible line was chosen, 307.590 nm. An important aspect in the direct analysis of solid samples is to achieve the determination of the analyte without dilution of the sample. Xenon short arc lamps emits a continuous high intensity spectrum exhibiting one of the highest luminance and radiance output of any continuously operating light source and very closely approach the ideal model for a point source of light. The high light intensity of the xenon short arc lamp provides an excellent signal-to-noise ratio for all wavelengths, enabling the use of less sensitive lines.

3.2. Optimization of the graphite furnace temperature programme

During the experiments in order to select the optimum wavelength was observed that while multiple peaks appeared for the eye shadow sample, only one peak was shown for ionic zinc and solid ZnO NPs standards. As has already been discussed in the introduction section, several researchers have observed different atomization profiles between ionic metals and their metallic NPs for Ag(I) and Ag NPs, Au(III) and Au NPs, Fe(II) and magnetic NPs; e.g. delayed atomization times for the NPs were always obtained [2,32–34]. Resano et al. [34] already stablished that the goal to separate ionic species from NPs was to maximize the difference between vaporization/atomization mechanisms as a function of the chemical species. For this reason, the optimization of the graphite furnace temperature programme was done by multiple response experiment designs whose responses were thought to maximize the difference between atomization profiles of Zn^{2+} and ZnO NPs. In a first central composite surface design, pyrolysis and atomization temperatures and atomization ramp were optimized, the three response functions selected tried maximize the height of the two peaks obtained during the eye shadow atomization and the distance between them. A 2^3 + star central composite design involving 16 experiments was selected. The ANOVA results produced graphs showing the standardized effects on the three response functions (pareto charts). The only statistically significant factor at the 95% confidence level ($p < 0.05$) was the atomization temperature, with a negative effect on the response function: height peak 1/mass. The multiple response surface obtained is shown in Fig. 1; as can be seen, with a low pyrolysis temperature (150 °C) and an atomization temperature from 1350 °C, the maximum desirability is achieved. Higher atomization temperature was not selected due to the negative effect on the first peak of the eye shadow. Thus, the optimal values selected for the three studied factors were: pyrolysis temperature, 150 °C; atomization ramp, 1000 °C s^{-1}; atomization temperature, 1350 °C.

A second 2^3 + star central composite design involving other 16 experiments was used for the optimization of the pyrolysis ramp, pyrolysis hold time and atomization hold time. However, now a single response function, distance between peaks, was considered, in order to avoid as much as possible, the overlap between them. The standardized pareto chart is shown in Fig. 2, the only factor statistically significant at the 95% confidence level was the pyrolysis ramp, with a negative effect on the response function. The optima values obtained from this design were: pyrolysis ramp, 3 °C/s; pyrolysis hold time, 6s; and atomization hold time, 3s. In Fig. 3 can be seen the response function surface. These results confirm that a slow pyrolysis (3 °C/s) at low temperature (150 °C) is essential to distinguish between ionic species and

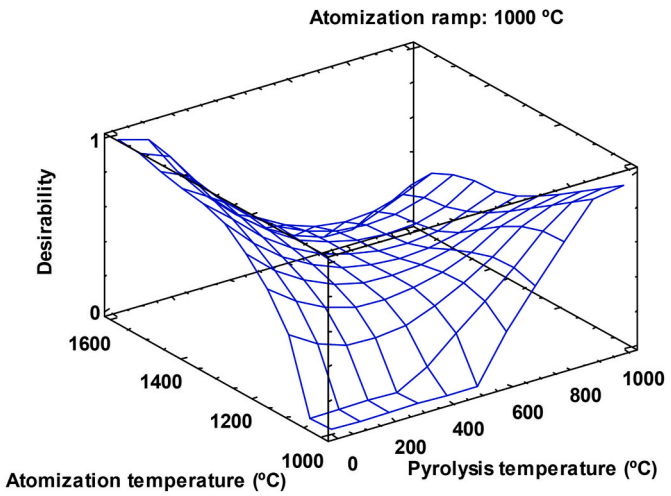

Fig. 1. Multiple response surface.

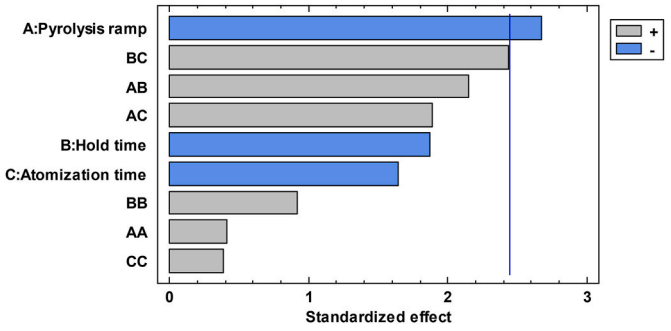

Fig. 2. Standardized Pareto chart for response distance between peaks.

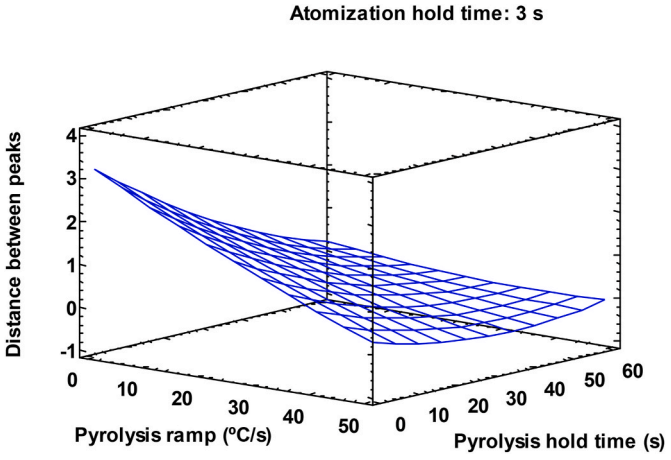

Fig. 3. Distance between peaks surface function.

nanoparticles of a same element. In Fig. 4 can be seen the spectra 3D and 2D obtained with the optimized conditions for a brown eye shadow. In order to assign each peak with its specie, the spectra of an aqueous standard of Zn(II) and a solid standard of ZnO NPs were separately registered, these spectra are showed in the same coordinate axes in Fig. 5. In this figure was observed that the first peak corresponded with $Zn^{2+}$and the second peak corresponded with ZnO NPs which is in agreement with that described in the literature [2,32–34]. On the other hand, the complete resolution of the peaks was not achieved, so to obtain a satisfactory quantification of mixtures of NPs and ionic species

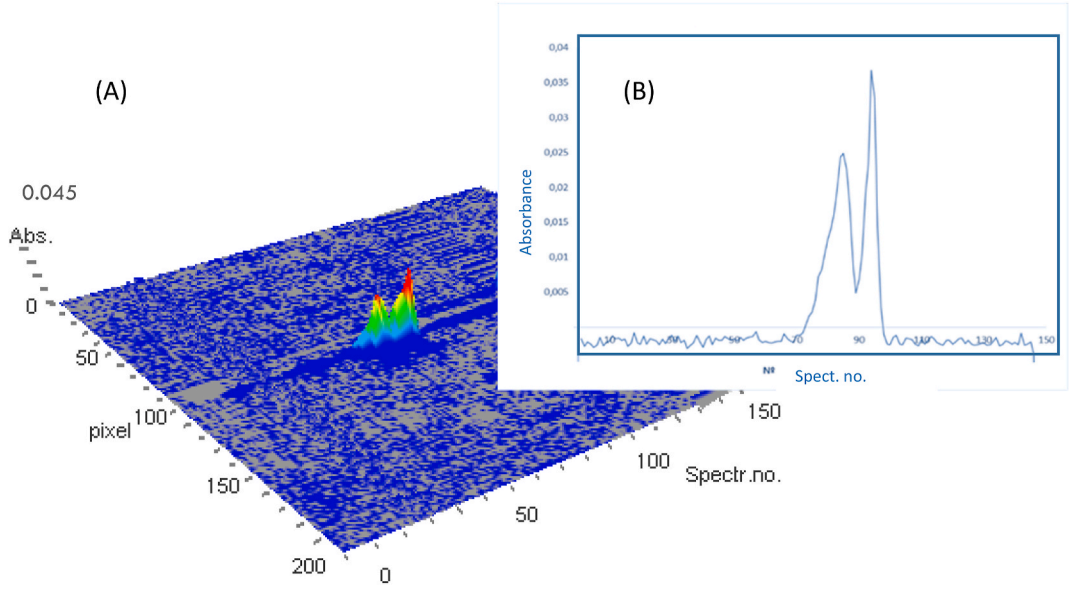

Fig. 4. 3D (A) and 2D (B) spectra of matt brown eye shadow. (For interpretation of the references to color in this figure legend, the reader is referred to the Web version of this article.)

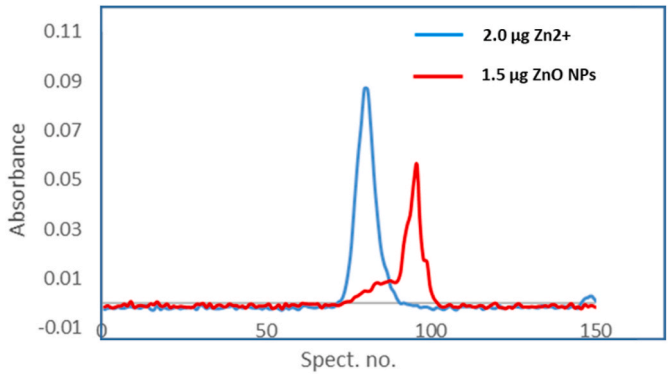

Fig. 5. 2D spectra of ionic zinc and ZnO NPs standards.

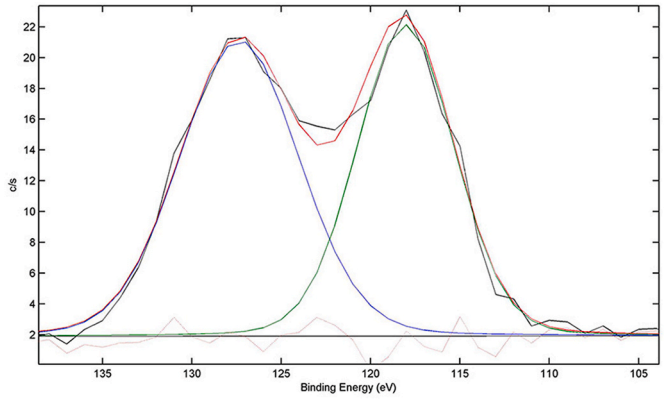

Fig. 6. Deconvoluted 2D spectrum of beige eye shadow. The units on the axes correspond with a XPS spectrum due to the Multipak software.

was necessary to properly deconvolute the two overlapping peaks. The deconvolution of the peaks was possible exporting the spectra data from instrument software, ASPECT CS, to CSV file format. Then, using a web service programmed in JavaScript, the pixel 101 was selected to represent the spectrum and the data were converted to a standard data transfer format for surface chemical analysis (ISO 14976:1998), compatible with Multipak software, where the deconvolution was made. A deconvoluted 2D spectrum for an eye shadow sample is shown in Fig. 6. On this way, a correct quantification of both species was accomplished. Must be noted that the units of the axes in the Fig. 6 correspond with a spectrum of X-Ray photoelectron spectroscopy (XPS) due to Multipak software belong to a XPS instrument, however the integrated areas have units of absorbance/spectr. no (time).

Additionally, experiments were performed to try determining the ZnO NPs size by means of the second atomization peak. For this, calibration curves were obtained with solid standards of ZnO NPs of different sizes (US Research Nanomaterials, Inc., Houston, USA). Two methodologies were tested, the measure of the upslope of the second peak of the atomization signals (atomization rate (k_{at})), and the time of appearance of its maximum height (atomization delay (t_{ad})). With both methodologies good calibration curves were obtained (Fig. 7). However, the results with the eyeshadow samples were highly non-reproducible, and they could not be validated by TEM. The reason is that the eyeshadow samples contain ZnO NPs with different sizes, in Fig. 8 the TEM micrograph of the matt brown eyeshadow is showed. Different sizes should produce atomization peaks at different times, but the difference between these times is not enough to be distinguished into the second atomization peak, even achieving its deconvolution.

Finally, in order to validate the speciation method, the analysis of total zinc was also addressed. Taking as starting point the results of the experiments of both designs above reported, several temperatures, ramps and hold times of pyrolysis and atomization were selected and tested in order to obtain an only atomization peak for Zn in the eye shadow samples. Finally, the best results were found for a temperature, ramp and hold time of pyrolysis of 300 °C, 50 °C/s and 20 s and a temperature, ramp and hold time of atomization of 1350 °C, 1500 °C/s and 3s, respectively. These results were shown in Table 1.

3.3. Performance of the method

Once the optima conditions were established, lineal calibration graphs were constructed with aqueous and solid standards separately, in order to calculate the performance of the method in both cases. The limits of detection (LOD) and quantification (LOQ) were calculated as the concentration of Zn^{2+}or ZnO NPs giving signals equivalent to three and ten times respectively, the standard deviation of the ordered at the

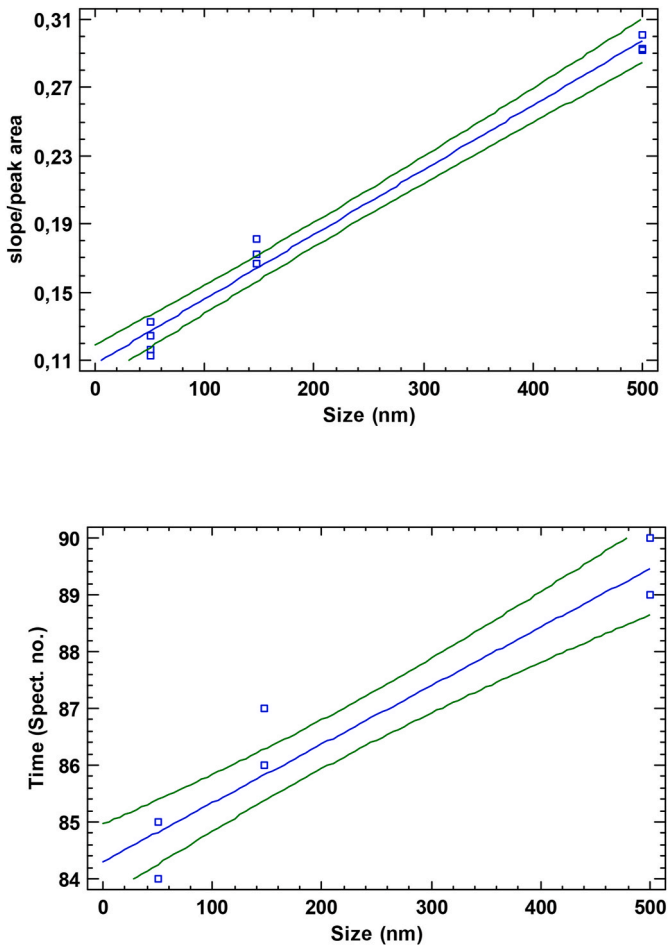

Fig. 7. Calibration graphs for ZnO NPs size by atomization rate (k_{at}) (A) and by atomization delay (t_{ad}) (B).

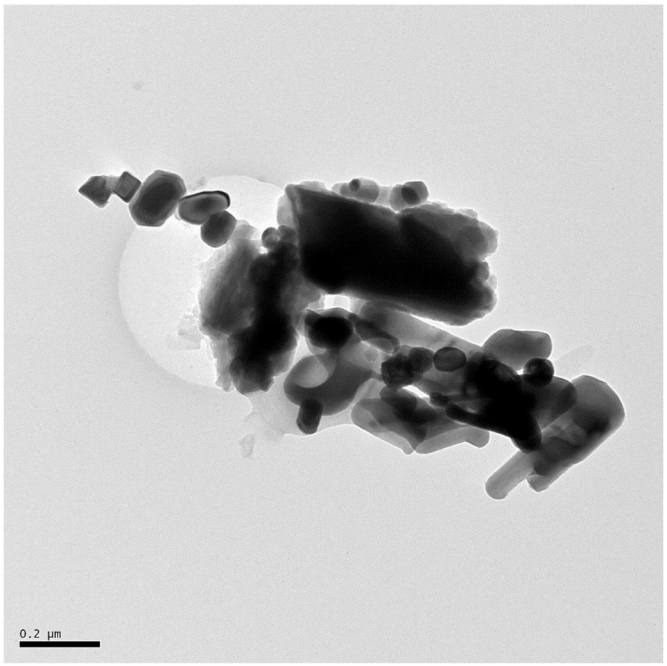

Fig. 8. TEM micrograph of matt brown eyeshadow sample.

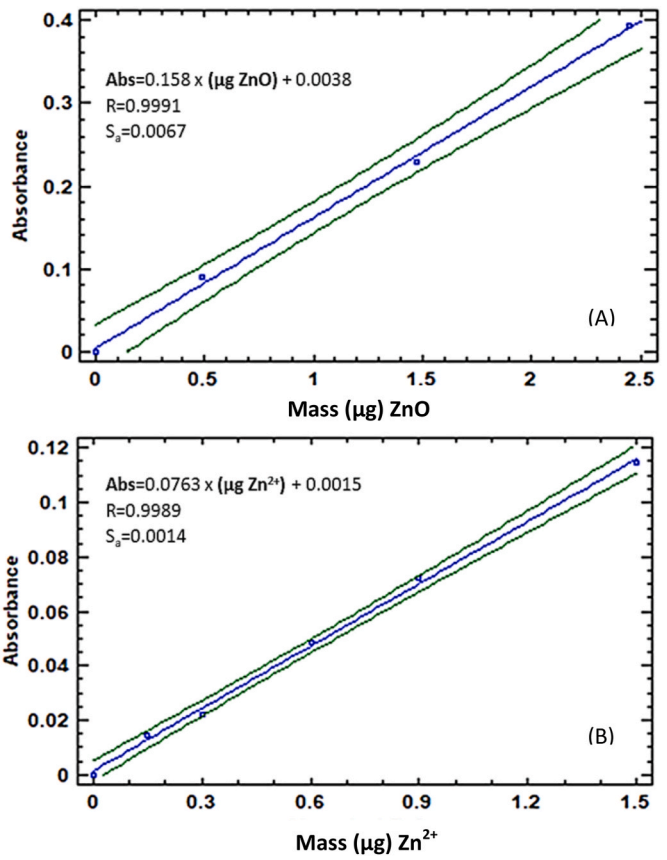

Fig. 9. Calibration graphs for ZnO NPs (A) and Zn^{2+}(B). S_a: standard deviation of the ordered at the origin.

origin of the calibration equation, because the blank signals and their standard deviations were too low and these quality parameters resulted with negative values. The calibration graphs, their linear regression equations, and the standard deviation of the ordered at the origin were reported in Fig. 9. The calculated LODs and LOQs were 0.06 and 0.18 µg Zn^{2+}, respectively; and 0.13 and 0.42 µg ZnO NPs, respectively, which are adequate for the analysis of these analytes in eyeshadow samples, being present concentrations of tenths of percent at eye shadow samples. These results might seem high for this technique (GFAAS). However, it must be remembered that the selected wavelength 307.590 nm, is around one hundred times less sensible than the principal, 213.857 nm. The precision was expressed as the percentage of the relative standard deviation (RSD). The RSD values calculated for ten replicates of 0.6 µg Zn^{2+} aqueous standard and ten replicates of 0.6 µg ZnO NPs were 2.5 and 6.9%, respectively.

3.4. Analytical application

In order to test the accuracy and applicability of the proposed method, five compact powder eye shadow samples of several brands and different colors were analysed. First, recovery assays of both species were realized. Recovery percentages between 98 and 115% were found for additions of different micro-aliquots of a 4 mg/L aqueous standard of Zn^{2+}, and between 80 and 100% for additions of different masses of a 0.049% solid standard of ZnO. The results of the recovery assays were given in Table 3. Second, the possibility of quantifying both species using calibration against aqueous or solid standards was explored, but probably due to low pyrolysis temperature used, the sample matrix was incompletely destroyed, thus the standard addition calibration method was used. The results of the speciation analysis of $Zn^{2+}$and ZnO NPs, both expressed as Zn percentage, were reported in Table 4.

Table 3
Recovery assays of $Zn^{2+}$and ZnO NPs.

	Added (μg)		Found (μg)		Recovery (%)	
	Zn^{2+}	ZnO NPs	Zn^{2+}	ZnO NPs	Zn^{2+}	ZnO NPs
Matt beige	–	–	0.093 ± 0.009	0.15 ± 0.02	–	–
	0.02	0.02	0.115 ± 0.014	0.17 ± 0.03	110	100
	0.04	0.04	0.132 ± 0.009	0.19 ± 0.05	98	100
Matt brown	–	–	0.26 ± 0.04	0.12 ± 0.02	–	–
	0.02	0.02	0.28 ± 0.04	0.14 ± 0.02	100	100
	0.04	0.05	0.30 ± 0.04	0.17 ± 0.02	100	100
Gloss brown	–	–	0.241 ± 0.002	0.61 ± 0.02	–	–
	0.02	0.02	0.262 ± 0.012	0.63 ± 0.02	105	100
	0.04	0.05	0.28 ± 0.06	0.65 ± 0.02	98	80
Gloss grey	–	–	0.237 ± 0.013	0.263 ± 0.014	–	–
	0.02	0.02	0.26 ± 0.08	0.28 ± 0.07	115	85
	0.04	0.04	0.278 ± 0.017	0.30 ± 0.07	103	93
Gloss purple	–	–	0.11 ± 0.03	0.16 ± 0.02	–	–
	0.02	0.02	0.13 ± 0.03	0.18 ± 0.03	100	100
	0.04	0.05	0.15 ± 0.04	0.21 ± 0.02	100	100

Table 4
Analysis of eye shadow samples.

	Zn content (%)				
	Zn^{2+}	ZnO NPs	Total (Zn^{2+}+ZnO)	Total Zn Direct SS	Total Zn Digested samples
Matt beige	0.043 ± 0.004	0.058 ± 0.007	0.101 ± 0.008	0.129 ± 0.009	0.101 ± 0.003
Matt brown	0.31 ± 0.02	0.11 ± 0.02	0.42 ± 0.03	0.478 ± 0.014	0.47 ± 0.03
Gloss brown	0.166 ± 0.002	0.33 ± 0.02	0.50 ± 0.02	0.50 ± 0.03	0.46 ± 0.09
Gloss grey	0.18 ± 0.02	0.153 ± 0.008	0.33 ± 0.02	0.30 ± 0.02	0.30 ± 0.09
Gloss purple	0.10 ± 0.03	0.102 ± 0.013	0.20 ± 0.03	0.26 ± 0.03	0.24 ± 0.13

SS: Solid sampling.
*All data are expressed in % of Zn^{2+}.

Besides of the recovery assays for both species, the total zinc was analysed by SS-HR CS-GFAAS using external calibration with aqueous standards of Zn^{2+} and the pyrolysis and atomization steps marked with an asterisk in Table 1. On the other hand, the eye shadow samples were also acid digested and analysed by the proposed temperature programme in the cookbook of the HR-CS-GFAAS CONTRAA 700 using aqueous standards of Zn^{2+}. The results of the total content of zinc as the sum of Zn^{2+}+ ZnO NPs, and the obtained for the two last analysis reported, all expressed as Zn percentage, were also reported in Table 4. The ANOVA analysis of the data on the three last columns in Table 4 showed that not significant differences existed between the results at 95% confidence level. Thus, both, the speciation method and the SS-HR-CS-GFAAS with aqueous standards were properly validated.

4. Conclusions

In this work has been demonstrated that simply changing the pyrolysis and atomization steps, by meaning of an adequate optimization of the temperature programme of the graphite furnace, it is possible to distinguish between ionic and NP forms of an element in a sample or to tackle the analysis of the total concentration of this element in that solid samples through a calibration with aqueous standards. Quantification of mixtures of ionic and NP forms require the proper deconvolution of the double peaks obtained. The SS-HR-CS-GFAAS developed methods enables the direct solid determination of Zn^{2+}, ZnO NPs and total Zn in eye shadow samples in a simple and straightforward way, carrying out the calibration for speciation analysis by the standard addition method, and the total content by external calibration with aqueous standards. The determination of the average size of the ZnO NPs by the use of the atomization delay for larger particles was not possible due the sizes heterogeneity of the ZnO NPs in eyeshadow samples.

The minimum sample manipulation (just a drying and homogenisation), avoiding the use of reagents, provides a facile, fast and green, analytical speciation method. It might be expected that similar methods could be extended to the speciation analysis of other elements in different types of samples.

Credit author statement

E.I. Vereda Alonso: Conceptualization, Methodology, Formal analysis, Writing - original draft, Writing - review & editing, Software, Data curation, Supervision, Resources, Funding acquisition. **M.M. López Guerrero**: Conceptualization, Methodology, Formal analysis, Writing - review & editing, Data curation, Supervision, Resources. **A. Rodríguez-Moreno**: Software. **P. Montoro Leal**: Investigation, Methodology, Writing - review & editing, Validation, Software, Formal analysis, Data curation. **J.C. García-Mesa**: Investigation, Methodology, Writing - review & editing, Validation, Software, Formal analysis, Data curation. All authors have read and agreed to the published version of the manuscript.

Declaration of competing interest

The authors declare that they have no known competing financial interests or personal relationships that could have appeared to influence the work reported in this paper.

Acknowledgements

This work has been partially supported by the University of Malaga (Proyecto Puente UMA), FEDER funds, Junta de Andalucia, Project UMA18FEDERJA060 and the Spanish Ministerio de Ciencia y Tecnologia (fellowship FPU18/05371).

References

[1] M.E. Vance T. Kuiken, E.P. Vejerano, S.P. McGinnis, M.F. Hochella, D. Rejeski, M. S. Hull, Nanotechnology in the real world: redeveloping the nanomaterial consumer products inventory, Beilstein J. Nanotechnol. 6 (2015) 1769–1780.

[2] N.S. Feichtmeier, N. Ruchter, S. Zimmermann, B. Sures, K. Leopold, A direct sampling analysis method for the detection of silver nanoparticles in biological matrices, Anal. Bioanal. Chem. 408 (2016) 295–305.

[3] A. Nel, T. Xia, L. Mädler, N. Li, Toxic potential of materials at the nanolevel, Science 311 (2006) 622–627.

[4] K.L. Aillon, Y. Xie, N. El-Gendy, C.J. Berkland, M.L. Forrest, Effects of nanomaterial physicochemical properties on in vivo toxicity, Adv. Drug Deliv. Rev. 61 (2009) 457–466.

[5] A. López-Serrano, R.M. Olivas, J.S. Landaluze, C. Cámara, Nanoparticles: a global visión. Characterization, separation, and quantification methods. Potential environmental and health impact, Anal. Methods 6 (2014) 38–56.

[6] S. Lee, X. Bi, R.B. Reed, J.F. Ranville, P. Herckes, P. Westerhoff, Nanoparticle size detection limits by single particle ICP-MS for 40 elements, Environ. Sci. Technol. 48 (2014) 10291–10300.

[7] A. Bour, F. Mouchet, J. Silvestre, I. Gauthier, E. Pinelli, Environmentally relevant approaches to assess nanoparticles ecotoxicity: a review, J. Hazard Mater. 283 (2015) 764–777.

[8] S. Barlow, A. Chesson, J.D. Collins, A. Flynn, A. Hardy, K.D. Jany, A. Knaap, H. Kuiper, J.C. Larsen, P. Le Neindre, J. Schants, J. Schlatter, V. Silano, S. Skerfving, P. Vannier, The potential risks arising from nanoscience and nanotechnologies on food and feed safety [1], EFSA J 958 (2009) 1–39.

[9] E.U. Verordnung (, Nr. 1169/2011 des Europäischen Parlaments un des Rates, 2011, pp. 1–46.

[10] A.I. Barros, T.V. Silva, E.C. Ferreira, J.A. Gomes Neto, Determination of lead in eye shadow and blush by high-resolution continuum source graphite furnace atomic absorption spectrometry employing direct solid sampling, J. Braz. Chem. Soc. 26 (2015) 140–146.

[11] A.R. Borges, A.T. Duarte, M. da L. Potes, M.M. Silva, M.G.R. Vale, B. Welz, Fluorine in eye shadow: development of method using high-resolution continuum source graphite furnace molecular absorption spectrometry via calcium mono-fluoride with direct solid simple introduction, Microchem. J. 124 (2016) 410–415.

[12] I. de la Calle, M. Menta, M. Klein, F. Séby, Screenig of TiO_2 and Au nanoparticles in cosmetics and determination of elemental impurities by multiple techniques (DLS, SP-ICP-MS, ICP-MS and ICP-OES), Talanta 171 (2017) 291–306.

[13] P.J. Lu, S.W. Fang, W.L. Cheng, S.C. Huang, M.C. Huang, H.F. Cheng, Characterization of titanium dioxide and zinc oxide nanoparticles in sunscreen powder by comparing different measurement methods, J. Food Drug Anal. 26 (2018) 1192–1200.

[14] J.W. Wiechers, N. Musee, Engineered inorganic nanoparticles and cosmetics: facts, issues, knowledge gaps and challenges 6 (2010) 408–431.

[15] OJEU. Regulation (EC), No 1223/2009 of the European Parliament and of the Council of 30 November 2009 on Cosmetic Products, 2009.

[16] I.C.C.R. Report, For International Cooperation on Cosmetic Regulation: 2011 Associations Survey of Nanomaterials Used in Cosmetic Products, 2011.

[17] A. Karhu, H.C. Dobourguier, From ecotoxicology to nanotoxicology, Toxicology 269 (2010) 105–119.

[18] H.L. Hooper, K. Jurkschat, A.J. Morgan, J. Bailey, A.J. Lawlor, D.J. Spurgeon, C. Svendsen, Comparative chronic toxicity of nanoparticle and ionic zinc to the earthworm Eisenia veneta in a soil matrix, Environ. Int. 27 (2011) 1111–1117.

[19] W. Zhang, Y. Zhao1, F. Li, L. Li1, Y. Feng, L. Min, D. Ma, S. Yu, J. Liu, H. Zhang, T. Shi, F. Li, W. Shen, Zinc oxide nanoparticle caused plasma metabolomic perturbations correlate with hepatic steatosis, Front. Pharmacol. 9 (2018) article 57.

[20] V.L. Pachapur, A.D. Larios, M. Cledón, S.K. Brar, M. Verma, R.Y. Surampalli, Review. Behaviour and characterization of titanium dioxide and silver nanoparticles in soils, Sci. Total Environ. 563–564 (2016) 933–943.

[21] S. Damayanti, T.N.B.T. Mat, P. Tiyasuwan, O. Bolcarovic, W. Yoo, A. B. Mahardhika, S. Jiranusornkul, Development and validation of atomic absorption spectroscopic method for analysis of ZnO in blemish balm cream, Chiang Mai J. Sci. 45 (2018) 404–412.

[22] G.A. Zachariadis, E. Sahanidou, Multi-element method for determination of trace elements in sunscreens by ICP-AES, J. Pharmaceut. Biomed. Anal. 50 (2009) 342–348.

[23] A. Salvador, M.C. Pascual-Artí, J.R. Adell, A. Requeni, J.G. March, Analytical methodologies for atomic spectrometric determination of metallic oxides in UV sunscreen creams, J. Pharmaceut. Biomed. Anal. 22 (2000) 301–306.

[24] A.I. Barros, D.V. de Babos, E.C. Ferreira, J.A. Gomes Neto, Effect of different precursors on generation of reference spectra for structural molecular background correction by solid sampling high-resolution continuum source graphite furnace atomic absorption spectrometry: determination of antimony in cosmetics, Talanta 161 (2016) 547–553.

[25] B. Bocca, G. Forte, F. Petrucci, A. Cristaudo, Levels of nickel and other potentially allergenic metals in Ni-tested comercial body creams, J. Pharmaceut. Biomed. Anal. 44 (2007) 1197–1202.

[26] N.M. Hepp, W.R. Mindak, J. Cheng, Determination of total lead in lipstick: development and validation of a microwave-assisted digestion, inductively coupled plasma-mass spectrometric method, J. Cosmet. Sci. 60 (2009) 405–414.

[27] E. Bolea-Fernandez, D. Leite, A. Rua-Ibarz, L. Balcaen, M. Aramendia, M. Resano, F. Vanhaecke, Characterization of SiO_2 nanoparticles by single particle-inductively coupled plasma-tandem mass spectrometry (SP-ICP-MS/MS), J. Anal At. Spectrom. 32 (2017) 2140–2152.

[28] K. Leopold, A. Philippe, K. Wörle, G.E. Schaumann, Analytical strategies to the determination of metal-containing nanoparticles in environmental waters, Trends Anal. Chem. 84 (2016) 107–120.

[29] I. Li, K. Leopold, Ligand-assisted extraction for separation and preconcentration of gold nanoparticles from waters, Anal. Chem. 84 (2012) 4340–4349.

[30] F. Gagné, P. Turcotte, C. Gagnon, Screening test of silver nanoparticles in biological samples by graphite furnace-atomic absorption spectrometry, Anal. Bioanal. Chem. 404 (2012) 2067–2072.

[31] M. Resano, M. Aramendia, M.A. Belarra, High-resolution continuum source graphite furnace atomic absorption spectromery for direct analysis of solid samples and complex materials: a tutorial review, J. Anal. At. Spectrom. 29 (2014) 2229–2250.

[32] E. Vereda Alonso, M.M. Lopez Guerrero, M.T. Siles Cordero, J.M. Cano Pavón, A. García de Torres, Characterization of solid magnetic nanoparticles by means of solid sampling high resolution continuum source electrothermal atomic absorption spectrometry, J. Anal. At. Spectrom. 31 (2016) 2391–2398.

[33] N.S. Feichtmeier, K. Leopold, Detection of silver nanoparticles in parsley by solid sampling high-resolution-continuum source atomic absorption spectrometry, Anal. Bioanal. Chem. 406 (2014) 3887–3894.

[34] M. Resano, E. García-Ruiz, R. Garde, High-resolution continuum source graphite furnace atomic absorption spectrometry for the monitoring of Au nanoparticles, J. Anal. At. Spectrom. 31 (2016) 2233–2241.

[35] J. Goupy, Plans d'Expériences Pour Surfaces de Réponse, Dunod, Paris, France, 1999.